http://dx.doi.org/10.5755/j01.eee.20.1.6160 ELEKTRONIKA IR ELEKTROTECHNIKA, ISSN 1392-1215, VOL. 20, NO. 1, 2014

Analysis and Modeling of Converter with PWM Output for Two-Phase Motor Applications

P. Zaskalicky[1], B. Dobrucky[2], M. Prazenica[2]
[1]*Faculty of Electrical Engineering & Informatics, Technical University of Kosice, Letna 9, 042 00 Kosice, Slovak Republic*
[2]*Faculty of Electrical Engineering,University of Zilina, Univerzitna 1, 010 26 Zilina, Slovak Republic*
branislav.dobrucky@fel.uniza.sk

***Abstract*—This paper presents a steady state analysis of two-phase voltage-source converters with pulse width modulation (PWM) and output voltage control for small two-phase motor drives. The mathematical models of the different converter connections are built on condition of assumption of idealized semiconductor devices. A complex Fourier series approach is used to predict to terminal voltage and current waveforms.**

***Index Terms*—Fourier series, mathematical model, two-phase converter, power conversion harmonics, pulse width modulation converters.**

I. INTRODUCTION

Electrical low-power drives (around 100 W) which are supplied by a single-phase voltage, used in different industrial and domestic devices, presently increasingly use two-phase motors [1]–[3]. Two-phase motors by their characteristics no differ from three-phase motors. Their advantage is easier winding, which is of great importance for automated production. The two-phase motors are manufactured as either squirrel cage asynchronous or permanent magnets synchronous motors. They are deployed as drive of pumps in a washing machines and dishwashers, but also as the circulating pumps for central domestic heating. A permanent magnet is in this case, water and lye resistant, allows making a pump with an absolute waterproof. Two-phase voltage is produced from the single-phase network using converters. The contribution deals with the various schemes of the two-phase inverters. Using the complex Fourier series is converter's output voltage mathematically expressed [4]–[8]. On the base of output voltages, the load currents are calculated for passive two-phase load.

For steady-state inverter's operation study we consider following idealized conditions [9]–[11]:

- Power switch, that means the switch can handle unlimited current and blocks unlimited voltage;
- The voltage drop across the switch and leakage current through switch are zero;
- The switch is turned on and off with no rise and fall times;
- Sufficiently good size capacity of the input voltage capacitors divider, to can suppose inverter input DC voltage to by constant [5], [9], [10].

Manuscript received March 26, 2013; accepted September 12, 2013.
This work was supported in part of the Slovak Research and Development Agency under the contract N0: APVV-0138-10.

This assumption helps us to analyse a power circuit and helps us to build a mathematical model of different concepts of two-phase converters.

II. TWO-PHASE CONVERTER USING HALF-BRIDGE CONNECTED INVERTER SCHEME

Figure 1 shows a scheme of two-phase converter with half-bridge connected inverter. Connecting to the network can be realized by different way with different types of devices [10].

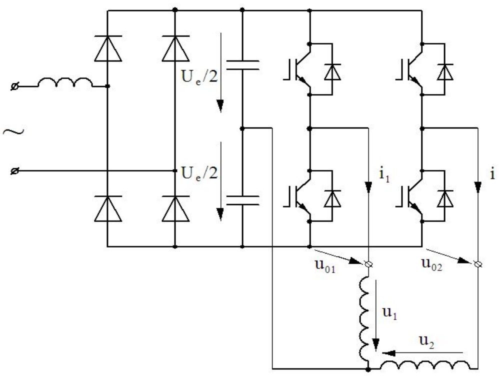

Fig. 1. Two-phase converter using half-bridge inverter.

An inverter consists of two transistor's branches, which form at the same time the output terminals of the converter. The load is connected between output terminals and the node of the capacitive voltage divider.

Power transistor each of branch can conduct only in the condition that the second branch transistor is blocked. Simultaneous transistors conducting creates a short circuit, simultaneous transistors blocking creates uncertain state.

In the case of upper transistor conducting, the branch voltage is equal to the DC input voltage (U_e). In the case of lower transistor conducting, the branch voltage is equal zero. Branch voltages can by the only positive value of voltage, either U_e or 0 value.

Assuming pulse-width modulation (PWM) of converter output voltage. PWM transform requested output voltage waveform to the series of impulsion of constant frequency and different width. Frequency of the output impulsion call modulated frequency.

Two parameters define the invertor control:

– *Coefficient of the modulation* m - equal to the ratio of the modulation and reference frequency;
– *Voltage control coefficient* r - equal to the ratio of the desired voltage amplitude and the DC supply voltage.

Generally to control the inverter numeric control device is used. The turn on ($\sim$) and turn off ( ) angles are calculated by the discredit of the reference sine-wave. That means the reference sine-wave is replaced by discrete values. If the coefficient of modulation m is sufficiently great, the difference between real values and discrete values is negligible.

The phase branches are control to create the output voltages as seen in:

$$u_{01} = \frac{U_e}{2} + r\frac{U_e}{2}\sin^{-}, \tag{1}$$

$$u_{02} = \frac{U_e}{2} + r\frac{U_e}{2}\cos^{-}, \tag{2}$$

where U_e -is a DC inverter's input voltage value.

Thus the requested phase voltages are given by:

$$u_1 = u_{01} - \frac{U_e}{2} = r\frac{U_e}{2}\sin^{-}, \tag{3}$$

$$u_2 = u_{02} - \frac{U_e}{2} = r\frac{U_e}{2}\cos^{-}. \tag{4}$$

To calculate a turn on ($\sim$) and turn off ( ) angles we use the approach comparing the DC impulse area with the reference voltage area [7]. For the first output transistors branch the following equations are valid:

$$\int_{\frac{2\text{®}}{m}\left(n-\frac{1}{2}\right)}^{n\frac{2\text{®}}{m}} \left(\frac{U_e}{2} + r\frac{U_e}{2}\sin^{-}\right) d^{-} = U_e\left(n\frac{2\text{®}}{m} - \sim_{01n}\right), \tag{5}$$

$$\int_{n\frac{2\text{®}}{m}}^{\frac{2\text{®}}{m}\left(n+\frac{1}{2}\right)} \left(\frac{U_e}{2} + r\frac{U_e}{2}\sin^{-}\right) d^{-} = U_e\left({}_{01n} - n\frac{2\text{®}}{m}\right). \tag{6}$$

After the calculus we obtain for the turn-on and turn-off angles of the first transistors branch the following expressions:

$$\sim_{01n} = \frac{\text{®}}{m}\left(2n - \frac{1}{2}\right) + \frac{r}{2}\left[\cos n\frac{2\text{®}}{m} - \cos\frac{\text{®}}{m}(2n-1)\right], \tag{7}$$

$$ {}_{01n} = \frac{\text{®}}{m}\left(2n + \frac{1}{2}\right) + \frac{r}{2}\left[\cos n\frac{2\text{®}}{m} - \cos\frac{\text{®}}{m}(2n+1)\right]. \tag{8}$$

It will be similar for the second transistor branch:

$$\sim_{02n} = \frac{\text{®}}{m}\left(2n - \frac{1}{2}\right) - \frac{r}{2}\left[\sin n\frac{2\text{®}}{m} - \sin\frac{\text{®}}{m}(2n-1)\right], \tag{9}$$

$$ {}_{02n} = \frac{\text{®}}{m}\left(2n + \frac{1}{2}\right) - \frac{r}{2}\left[\sin n\frac{2\text{®}}{m} - \sin\frac{\text{®}}{m}(2n+1)\right]. \tag{10}$$

Then we can write the output voltage of the first branch in the form of a complex Fourier series [1], [4]:

$$u_{01} = rU_e \sum_{k=-\infty}^{\infty}\sum_{n=1}^{m} c_{01n} e^{jk^{-}}, \tag{11}$$

where $c_{01n} = \frac{1}{j2k\text{®}}\left(e^{-jk\sim_{01n}} - e^{-jk\ \ {}_{01n}}\right)$, *for* $k \neq 0$ and

$c_{01n} = \frac{ {}_{01n} - \sim_{01n}}{2\text{®}}$, *for* $k = 0$.

Similarly for the output voltage of the second transistor branch

$$u_{02} = rU_e \sum_{k=-\infty}^{\infty}\sum_{n=1}^{m} c_{02n} e^{jk^{-}}, \tag{12}$$

where $c_{02n} = \frac{1}{j2k\text{®}}\left(e^{-jk\sim_{02n}} - e^{-jk\ \ {}_{02n}}\right)$, *for* $k \neq 0$ and

$c_{02n} = \frac{ {}_{02n} - \sim_{02n}}{2\text{®}}$, *for* $k = 0$.

Figure 2 depicts the calculated branch voltage waveform, calculated on the base of (9), (10) and (11). Requested output frequency is $f = 50\,Hz$, modulation $m = 30$ and voltage control coefficient $r = 1$.

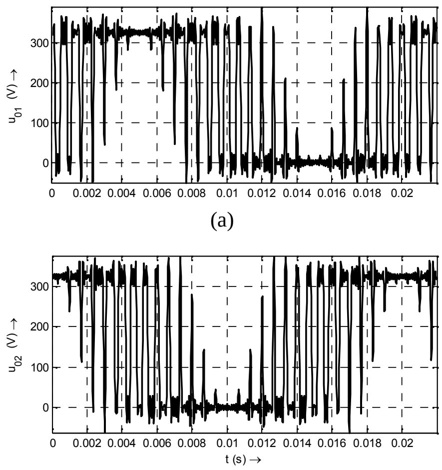

(a)

(b)

Fig. 2. Branch output voltage waveforms: phase.

For the phase voltages, the following are valid:

$$u_1 = u_{01} - \frac{U_e}{2} = rU_e \sum_{k=-\infty}^{\infty}\sum_{n=1}^{m} c_{01n} e^{jk^{-}} - \frac{U_e}{2}, \tag{13}$$

$$u_2 = u_{02} - \frac{U_e}{2} = rU_e \sum_{k=-\infty}^{\infty}\sum_{n=1}^{m} c_{02n} e^{jk^{-}} - \frac{U_e}{2}. \tag{14}$$

There are phase voltages waveforms shown in the Fig. 3. The voltages are bipolar with amplitude equal to half of DC input voltage.

For the phase output current we obtain the following relation:

$$i_1 = rU_e \sum_{k=-\infty}^{\infty}\sum_{m=1}^{p} c_{01n} \frac{e^{jk^{-}}}{R + jk\mu L} - \frac{U_e}{2R}, \tag{15}$$

$$i_2 = rU_e \sum_{k=-\infty}^{\infty}\sum_{m=1}^{p} c_{02n} \frac{e^{jk^{-}}}{R + jk\mu L} - \frac{U_e}{2R}. \tag{16}$$

Figure 4 depicts the phase output current waveforms, calculated on the base of (13), (14).

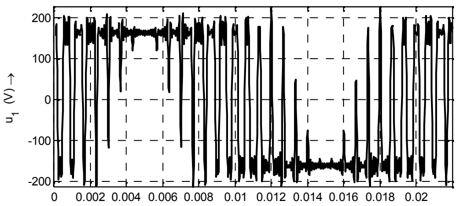

(a)

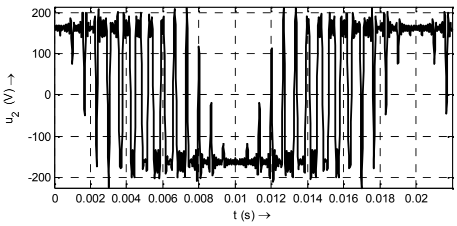

(b)

Fig. 3. Phase voltages output waveforms: phase.

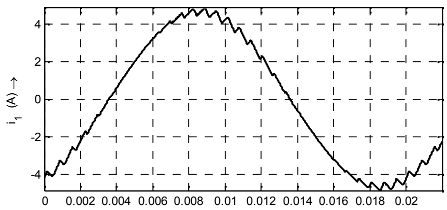

(a)

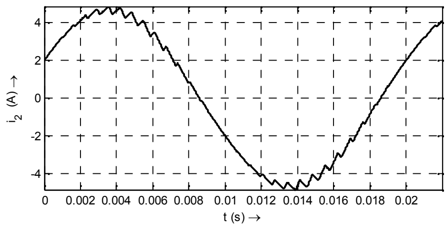

(b)

Fig. 4. The phase current waveforms: phase a) -top and b) -bottom.

The current waveforms were calculated for the passive ohm-inductive load of $R = 15\Omega, L = 100\,mH$.

III. Two-Phase Converter Using a Three-Phase Half-Bridge Inverter Scheme

Figure 5 shows a scheme of two-phase converter with bridge 3-phase inverter. The inverter of the converter consists of three transistors branches. The first branch is common branch for both phases. The load is connected to the each phase terminal nodes, and next connected to the centre of the first branch. The advantage compared to the half-bridge connection is that there is not necessary to create capacitive divider. Maximum output voltage is of $\sqrt{2}$ higher than in the case of half-bridge connection.

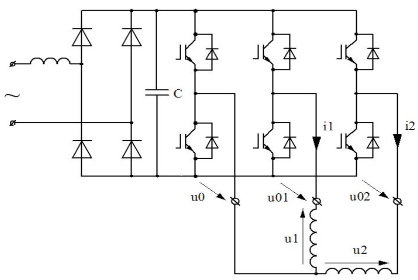

Fig. 5. Two-phase converter using 3-phase bridge inverter.

The control of three branches instead of two is rather complicated, what increase realization fee as well as complexity of inverter hardware due to six transistors. In this case required output voltage of the branches has a form:

$$u_0 = \frac{U_e}{2} + r\frac{U_e}{2}\sin^{-}, \tag{17}$$

$$u_{01} = \frac{U_e}{2} + r\frac{U_e}{2}\cos^{-}, \tag{18}$$

$$u_{02} = \frac{U_e}{2} - r\frac{U_e}{2}\cos^{-}. \tag{19}$$

Thus the requested phase voltages are given by:

$$u_1 = u_0 - u_{01} = r\frac{U_e}{\sqrt{2}}\sin\left(^{-} - 45^\circ\right), \tag{20}$$

$$u_2 = u_0 - u_{02} = r\frac{U_e}{\sqrt{2}}\cos\left(^{-} - 45^\circ\right). \tag{21}$$

For positive cosine and sine function (7)–(10) are valid. For the negative cosine function for turn-on and turn-off angles the following equations were developed:

$$\sim_{02n} = \frac{\circledR}{m}\left(2n - \frac{1}{2}\right) + \frac{r}{2}\left[\sin n\frac{2\circledR}{m} - \sin\frac{\circledR}{m}(2n-1)\right], \tag{22}$$

$$_{02n} = \frac{\circledR}{m}\left(2n + \frac{1}{2}\right) + \frac{r}{2}\left[\sin n\frac{2\circledR}{m} - \sin\frac{\circledR}{m}(2n+1)\right]. \tag{23}$$

We can express the branch voltages in a form of complex Fourier series:

$$u_0 = rU_e \sum_{k=-\infty}^{\infty}\sum_{n=1}^{m} c_{0n} e^{jk^{-}}, \tag{24}$$

$$u_{01} = rU_e \sum_{k=-\infty}^{\infty}\sum_{n=1}^{m} c_{01n} e^{jk^{-}}, \tag{25}$$

$$u_{02} = rU_e \sum_{k=-\infty}^{\infty}\sum_{n=1}^{m} c_{02n} e^{jk^{-}}. \tag{26}$$

The phase voltages a given by a difference of branch voltages:

$$u_1 = u_0 - u_{01} = rU_e \sum_{k=-\infty}^{\infty}\sum_{n=1}^{m} \left(c_{0n} - c_{01n}\right) e^{jk^{-}}, \tag{27}$$

$$u_2 = u_0 - u_{02} = rU_e \sum_{k=-\infty}^{\infty}\sum_{n=1}^{m} \left(c_{0n} - c_{02n}\right) e^{jk^{-}}. \tag{28}$$

There are the phase voltage waveforms shown in the Fig. 6, which were calculated on the base on (27) and (28).

The phases current are given by a formula:

$$i_1 = rU_e \sum_{k=-\infty}^{\infty}\sum_{m=1}^{p} \left(c_{0n} - c_{01n}\right) \frac{e^{jk^{-}}}{R + jk\mu L}, \tag{29}$$

$$i_2 = rU_e \sum_{k=-\infty}^{\infty}\sum_{m=1}^{p} \left(c_{0n} - c_{02n}\right) \frac{e^{jk^{-}}}{R + jk\mu L}. \tag{30}$$

Figure 7 depicts the phase output current waveforms, calculated on the base of (29) and (30).

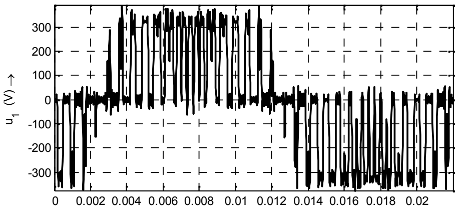

(a)

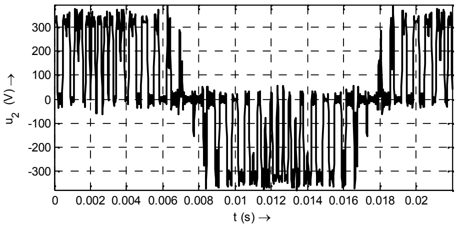

(b)

Fig. 6. Phase voltages output waveforms.

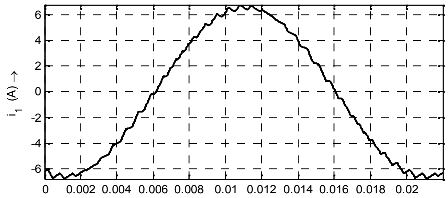

(a)

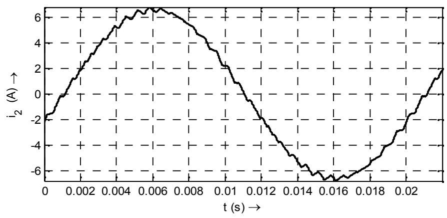

(b)

Fig. 7. The phase current waveforms: phase.

As in previous case the current waveforms were calculated for the passive ohm-inductive load of R = 15 Ω, L= 100 mH.

IV. EXPERIMENTAL VERIFICATION

Result of experimental measurements are shown in the Fig. 8.

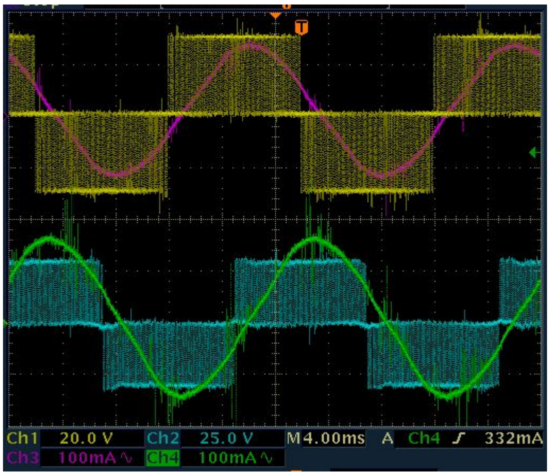

Fig. 8. Worked-out waveforms of the phase voltages (yellow, blue) and currents (pink, green) of two-phase bridge inverter: phase a) -top and b) -bottom.

The results in Fig. 8 were worked-out by experimental measurements on test rig with two-phase bridge 3-phase inverter (see Fig. 5) with parameters:

DC link voltage 50 V; R = 15 Ω; L= 100 mH;

Fundamental frequency 50 Hz;

Frequency modulation index m = 30.

V. CONCLUSIONS

Modelling, analysis, and of the two-phase PWM controlled converter were provided and presented in the paper. The developed equations in the form of a complex Fourier series for each inverter connection are valid for any coefficient of modulation, frequency and voltage control coefficients.

Simulation results of two differ type of inverter (half-bridge and full-bridge) are given. The experimental results in Fig. 8 are comparable to those in Fig. 6 and Fig. 7, respectively.

Advantages of this converter compare to the precedent half bridge connection is except of $\sqrt{2}$ higher maximal output voltage also higher quality of output current (minimized ripple, THD, etc.). That is mostly favorable for motor applications when operating in region of high speed and calling for higher ‘smooth’ supply currents, e.g. [7].

REFERENCES

[1] B. Dobrucky, P. Spanik, M. Kabasta, “Power electronics two-phase orthogonal system with HF input and variable output”, *Elektronika ir elektrotechnika (Electronics and Electrical Engineering)*, Kaunas: Technologija, 2009, no. 1, pp. 9–14.

[2] S. Kascak, P. Zaskalicky, B. Dobrucky, M. Prazenica, “Two-phase space vector modulation of FOC controlled ASM fed by 2-phase VSI inverter”, in *Proc. of EPE/PEMC 15th Int’l Conference*, Novi Sad (RS): IEEE Publisher, 2012, p. 5. CD ROM.

[3] P. Zaskalicky, “Modeling of converters with PWM control of output voltage for small two-phase drives”, in *Proc. of ICLVEM 12th Int’l Conference*, Brno (CZ), 2012, p. 5. CD ROM.

[4] M. Zaskalicka, P. Zaskalicky, M. Benova, M.A.R. Abdalmula, B. Dobrucky, “Analysis of Complex Time Function of Converter Output Quantities Using Complex Fourier Transform/Series”, *Communications - Scientific Letters of the University of Zilina*, 2010, no. 1, vol. 12, pp. 23–30.

[5] M. Marcokova, “Equiconvergence of two Fourier series”, *Journal of Approximation Theory*, Elsevier, 1995, vol. 80, no. 2, pp. 151–163. [Online]. Available: http://dx.doi.org/10.1006/jath.1995.1012

[6] B. Dobrucky, M. Benova, P. Spanik, “Using complex conjugated magnitudes- and orthogonal Park-Clarke transformation methods of DC/AC/AC frequency converter”, *Elektronika ir elektrotechnika (Electronics and Electrical Engineering)*, Kaunas: Technologija, 2009, no. 5, pp. 29–33.

[7] P. Zaskalicky, B. Dobrucky, “Complex Fourier series mathematical model of a three-phase inverter with improved PWM output voltage control”, *Elektronika ir elektrotechnika (Electronics and Electrical Engineering)*, Kaunas: Technologija, 2012, no. 7, pp. 65–68.

[8] M. Marcokova, V. Guldan, “On one orthogonal transform applied on a system of orthogonal polynomials in two variables”, n *Proc. of APLIMAT 8th Int’l Conference*, Bratislava (SK), STU Publisher, 2009, pp. 621–626.

[9] H. Buhler, *Power Electronics* (*Électronique de puissance)*, Laussane, CH (Switzerland): Traité d’électricité, 1987, chaps. 2–4. (in French)

[10] N. Mohan, T. M. Undeland, W. P. Robbins, *Power Electronics: Converters, Applications, and Design, 2nd ed.*, John Wiley & Sons, Inc. (NY), 1993, chaps. III–VI.

[11] S. Jeevananthan, P. Dananjayan, R. Madhavan, “Novel Single-Phase to Single-Phase Cycloconversion Strategies: Mathematical and Simulations Studies”, *Int’l Journal of Power and Energy Systems,* ACTA Press (CA), vol. 27, no. 4, pp. 414–423, 2007.